The role of Fusarium oxysporum effector protein Avr2 in resistance and pathogenicity

Ma, L.

Publication date
2012

CHAPTER 4

Subcellular localization and structure-function analyses of *Fusarium oxysporum* effector Avr2

Abstract

To promote host colonization plant pathogens secrete effector proteins. Recognition of these effectors by plant resistance proteins triggers resistance responses halting pathogen ingress. Hence, effectors play key roles in pathogenicity and resistance. Effector Avr2 from *Fusarium oxysporum* f. sp. *lycopersici* (*Fol*) is a small protein able to activate intracellularly the cytosolic tomato I-2 resistance protein. Here, we show that expression of *AVR2* is strongly induced in root- and xylem-colonizing hyphae three days post inoculation. Local accumulation of Avr2, in discrete structures of unknown identity, is observed alongside the fungal hyphae upon *Fol* infection of tomato roots. Using heterologous expression systems we found that Avr2 has to be nuclear localized to trigger an *I-2*-dependent cell death response. Subsequent structure-function analyses of Avr2 demonstrated that, except for the N-terminal 17 amino acids, the entire protein is required for I-2-mediated recognition. Avr2 forms homodimers in *planta*, but dimerization alone is insufficient to activate I-2 signalling.

A manuscript is prepared as:
L. Ma, B.J.C. Cornelissen and F.L.W. Takken

Introduction

Many plant pathogens secrete small proteins into the intercellular spaces or directly into host cells to facilitate infection and colonization of their hosts (Ellis *et al.*, 2009; Tyler, 2009). These proteins are referred to as effectors and they play roles to the benefit of the pathogen, such as manipulating host cell structure and interfering with essential biological processes of the host to aid infection (Alfano, 2009; Kamoun, 2006). The best-studied effectors come from bacterial pathogens such as *Pseudomonas syringae,* that frequently employ type III secretion systems to directly deliver effectors into the cytosol (Shames and Finlay, 2012). Filamentous plant pathogens lack a type III secretion system and secrete their effectors directly into the intercellular spaces like the apoplast or the xylem vessels. Haustorium-forming pathogens typically secrete their effectors in the periplasmic space. The secreted effectors can than either be taken up by the host cell, or exert their functions in the intercellular spaces (Koeck *et al.*, 2011; Stergiopoulos and de Wit, 2009). The mechanism by which fungal and oomycete effectors enter host cell is as yet unknown, but our understanding of the function of these effectors is growing (Stergiopoulos and de Wit, 2009).

To counteract the action of effectors plants evolved immune receptors, also called resistance (R) proteins, that perceive the presence or actions of these effectors (Chisholm *et al.*, 2006; Maekawa *et al.*, 2011). Perception of a specific effector by a corresponding R protein leads to activation of effector-triggered immunity (ETI), a response that is typically associated with programmed cell death of the infected cells. The induced resistance responses restrict further outgrowth of the pathogen at the infection site (Spoel and Dong, 2012). An effector recognized by a corresponding R protein is called an avirulence or Avr protein. The genetic interaction between an *AVR* and *R* gene pair has been described in the 40's by Flor, and is referred to as the gene-for-gene model (Flor, 1942). Many pairs of *AVR* and *R* genes have been identified and characterized (Gassmann and Bhattacharjee, 2012). The major class of intracellular R proteins is found to contain a central nucleotide-binding (NB) domain fused to a C-terminal leucine-rich repeat (LRR) region. At their N-terminus these NB-LRR proteins often carry a domain that either contains predicted coiled-coil motifs (CC-NB-LRR proteins) or that has homology to the Toll/interleukin-1 receptor (TIR-NB-LRR proteins) (Lukasik and Takken, 2009; Takken and Tameling, 2009). To overcome resistance genes pathogens can either mutate or shed the recognised effector, or develop new effectors that avoid or suppress recognition of the latter by the *R* gene (Stergiopoulos and de Wit, 2009). Concomitantly, plants continuously need to develop novel R proteins recognizing these novel/modified effectors, resulting in a co-evolutionary arms-race between pathogens and their hosts (Jones and Dangl, 2006) (Stergiopoulos and de Wit, 2009). Our understanding of the molecular basis underlying pathogenicity and resistance increased tremendously over the last decade (Spoel and Dong, 2012). However, most of our insights are based on studies of bacterial pathosystems and those on fungal and oomycetes are

lagging behind. This is a reason for concern since not bacterial but mainly fungal and fungal-like diseases are jeopardizing our food security and are responsible for some of the most severe diseases and even extinctions of wild species (Fisher *et al.*, 2012). Because of practical reasons most studies are performed using leaf-invading pathogens, while actually the root-invading vascular diseases pose a much bigger treat to agriculture since these are much more difficult to control. Hence a better understanding of how the plant immune system perceives this type of fungal pathogens is crucial. Here, we focus on the xylem-colonizing fungus *Fusarium oxysporum* f.sp. *lycopersici* (*Fol*) and its host tomato. Besides being an excellent pathosystem to study pathogenesis it is also perfectly adapted to study resistance mechanisms since the interaction complies with the gene-for-gene model.

Fusarium oxysporum is a soil-born, asexual fungus. The species complex contains many plant pathogens that can cause vascular wilt diseases in a wide variety of hosts by colonizing their xylem vessels (Di Pietro *et al.*, 2003; Michielse and Rep, 2009). Based on its host specificity, *F. oxysporum* is classified into so-called *formae speciales*, such as the tomato infecting *F. oxysporum* f.sp. *lycopersici* (*Fol*) strain, *F. oxysporum* f.sp. *melonis* (*Fom*) infecting melon and *F. oxypsorum* f.sp. *cubense* (*Foc*) invading banana (Michielse and Rep, 2009) (armstrong and Armstrong, 1981). Not all hosts are equally susceptible and some of them carry resistance genes against *Fusarium*. The *Fol* R genes in tomato are called 'immunity' or "*I*" genes. So far, three *I* genes, named *I* (or *I-1*), *I-2* and *I-3* conferring resistance against *Fol* races harbouring the corresponding *AVR* genes, have been introgressed from resistant *Solanum* species into cultivated tomato. Only *I-2* has been cloned and found to encode a classical NB-LRR protein. Studies using an *I-2* promoter fused to the β-glucuronidase (*GUS*) reporter gene revealed that *I-2* is specifically expressed in the parenchyma cells adjacent to the xylem vessels (Mes *et al.*, 2000). The subcellular localisation of I-2 is as yet unknown. Typically activation of an NB-LRR resistance protein induces a programmed cell death response of the infected cells. However, *I-2*-mediated resistance seems to be distinct, as the defence response typically does not induce cell death. *Fol* recognition leads to specific responses in the parenchymal cells as the xylem itself does not contain living tissue. These responses include accumulation of phenolics, callose deposition, and formation tyloses (outgrowth of xylem contact cells) and gels in the infected vessels (Takken and Rep, 2010; Beckman, 2000).

Xylem sap proteome analysis of the interaction between *Fol* and tomato resulted in identification of the *Fol* AVR2 protein. The *AVR2* gene encodes a 15.7 kDa mature protein (after cleavage of the predicted N-terminal signal peptide), which does not show similarity to other known proteins (Houterman *et al.*, 2009). Further studies revealed that Avr2 has a dual function: as a virulence factor it is required for full pathogenicity on susceptible plants, and as an avirulence determinant it triggers resistance in tomato carrying the *I-2* resistance gene. Some *I-2* mediated resistance-breaking *Fol* strains carry point mutations in *AVR2* preventing

its recognition by *I-2*. Co-expression of *I-2* and such a mutant in either tomato or in leaves of *Nicotiana benthamiana* does not induce a visual defence response. Although Avr2 is secreted into the xylem sap upon *Fol* infection, the Avr2 protein can activate I-2 intracellularly to trigger cell death in both *Nicotiana benthamiana* and tomato, implying its uptake into plant cells (Houterman *et al.*, 2009). Studies from Kale and co-workers have shown that an "RXLR-like" motif, represented by the "RIYER" sequence in Avr2, could play a role in entry of this effector in plant cells (Kale *et al.*, 2010). However, in the Kale study a truncated Avr2 protein, encompassing only the N-terminal part of the protein, was utilized for the uptake assays and uptake of full length Avr2 protein has not been assessed.

In chapter 6 it is shown that *Agrobacterium*-mediated expression of an Avr2 variant, of which the signal peptide for secretion has been deleted, localizes both in the cytoplasm and inside the nucleus. However, currently, it is unclear in which specific cell compartment, cytoplasm or nucleus, I-2 perceives Avr2 to trigger cell death. Also it is unknown at what stage of infection *AVR2* is expressed by the fungus to allow its *I-2*-mediated recognition and subsequent induction of host defences. In this study, we investigated the *in planta* expression of *AVR2* during the infection process. We also examined the subcellular localization of Avr2 both in heterologous expression systems and in tomato roots following *Fol* infection. Finally, we performed structure-function analyses of Avr2 to identify the minimal region and functional constraints of the effector that are required to activate I-2 signalling.

Results

AVR2 is predominantly expressed in xylem-colonizing fungal hyphae

To determine at which stage of infection *AVR2* is expressed, a *Fol* strain carrying an *AVR2*-promoter-reporter construct was created. Monomeric red fluorescent protein (mRFP) was used as reporter protein and the p*AVR2:RFP* construct was transformed into a Fol-p*AVR3:GFP* recipient strain. In this strain *AVR3* has previously been replaced by *GFP* encoding the Green Fluorescent Protein (van der Does *et al.*, 2008). The advantage of employing the Fol-p*AVR3:GFP* strain is that GFP can be used to monitor the growth of *Fol* in roots as the *AVR3* gene is specifically induced upon colonisation of the tomato roots (van der Does *et al.*, 2008). The p*AVR2*:*RFP* construct was designed to integrate by homologous recombination into the *AVR2* locus (see material and methods) to exclude differences in expression due to position effects. Out of the 150 hygromycin resistant transformants one genuine *AVR2* replacement mutant was identified based on the absence of *AVR2* and the insertion of *mRFP* and the hygromycin cassette in the *AVR2* locus (data not shown). This transformant was used to inoculate ten-day-old tomato seedlings according to the root-dip

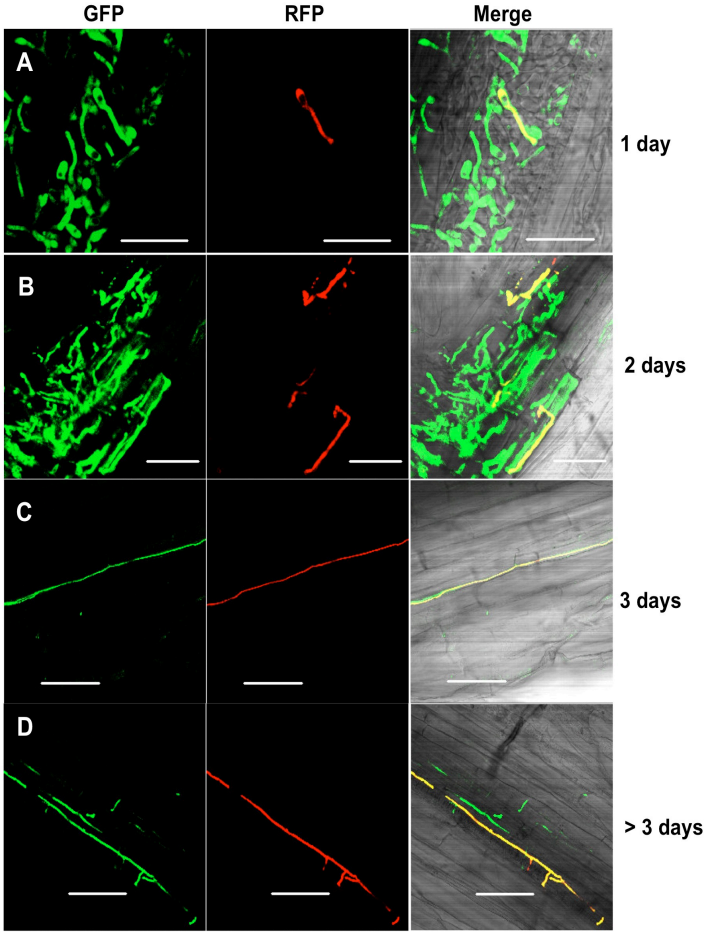

Figure 1. Infection process of *Fol* p*AVR2:RFP* and Fol p*AVR3:GFP* on tomato roots. RFP and GFP fluorescence was visualized using confocal microscopy. Imagines are depicted as separate red and green channels and as a merged figure. Ten-day-old tomato seedlings were inoculated with a *Fol* spore suspensions and roots were analysed at different time points post inoculation. **A)** One day after inoculation germinating spores can be found on the surface of tomato roots. **B)** Two days after inoculation hyphae have penetrated the epidermis and start to grow between the cortical cells. **C)** Three days after inoculation hyphae are growing between cortical cells. **D)** After three days, hyphae grow inside the xylem vessels. White scale bars represent 25 μm.

plate method (van der Does *et al.*, 2008). Expression of both reporter genes was studied in a time-course analysis by visualizing the RFP and GFP signals in inoculated roots using confocal microscopy. Figure 1A shows that, at one-day post inoculation, only few of the germinated spores displays RFP florescence, whereas a GFP signal is present in most of the germinating spores. This difference in expression confirms the observation that *AVR3* is induced upon contact with tomato roots (van der Does *et al.*, 2008), and reveals that in the majority of fungal biomass colonising the root cortex Avr2 is not expressed. Two days after inoculation an RFP signal was still only detectable in a very limited number of hyphae or spores that show GFP fluorescence (Figure 1B). At three days after inoculation red fluorescence was visible in some of the GFP fluorescent hyphae growing between the cortical cells (Figure 1C), but the majority of the green fluorescent hyphae does not show red

fluorescence. Four days after inoculation, RFP and GFP double fluorescent fungal hyphae can frequently be found growing inside xylem vessel (Figure 1D), demonstrating that *AVR2* is highly expressed at this stage of infection. From these observations we conclude that upon contact with tomato roots and during early stages of infection expression of *AVR3* precedes that of *AVR2*. Three days after inoculation high expression of both *AVR3* and *AVR2* is found in hyphae growing in the xylem vessels of tomato roots. So, although there are similarities, there are also distinct differences in the expression patterns of these two avirulence genes during root colonisation.

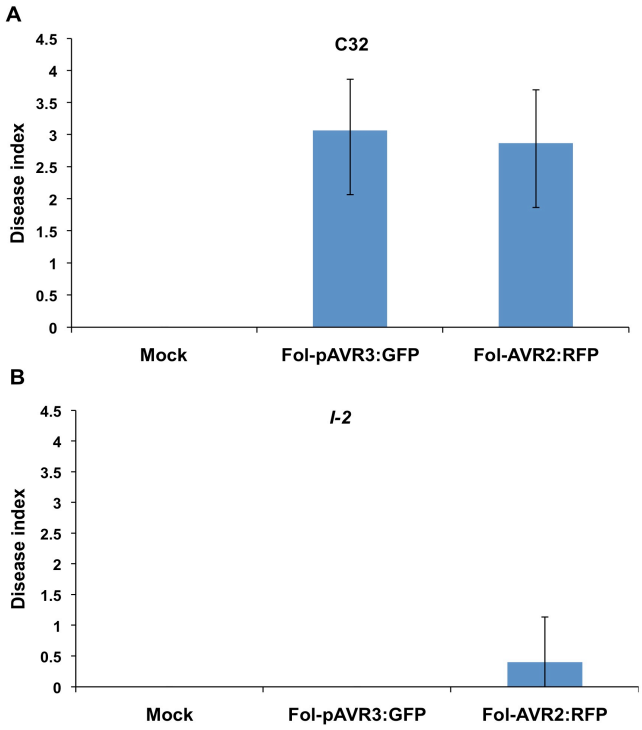

Figure 2. Fol-*AVR2:RFP* causes disease on susceptible tomato plants but not on resistant *I-2* plants. Ten-day-old tomato seedlings were inoculated with a *Fol* spore suspension using root-dip inoculation. Disease symptom (disease index ranging from 0 to 4) was scored three weeks after inoculation. Error bars indicate standard deviation. **A)** Average disease index of 20 plants three weeks after mock inoculation (water) or inoculation with either Fol-p*AVR3:GFP* or Fol-*AVR2:RFP* on susceptible C32 plants. **B)** Average disease index of 20 plants three weeks after mock inoculation (water) or inoculation with either Fol-p*AVR3:GFP* or Fol-*AVR2:RFP* on *I-2* plants.

Avr2 accumulates in spot-like structure upon *Fol* infection of tomato roots

Since in heterologous systems Avr2 activates I-2 intracellularly and triggers cell death, we speculate that Avr2 is also translocated into plant cells during *Fol* colonization. To examine the *in planta* localisation of Avr2 during *Fol* infection, we generated *Fol* transformants analogously as described above. However, instead of just the *RFP* gene a p*AVR2*:*AVR2*:*RFP* fusion gene was introduced in the Fol-*pAVR3:GFP* strain. Out of the 800 hygromycin resistant transformants three independent *AVR2* replacement mutants were

identified by PCR based on the insertion of p*AVR2*:*AVR2:RFP* and the hygromycin cassette in the *AVR2* locus (data not shown).

To assess the functionality of the fusion protein, we first tested whether the p*AVR2*:*AVR2:RFP* containing transformants can still cause disease on susceptible plants and trigger *I-2*-mediated resistance on resistant cultivars. Thereto, ten-day-old tomato seedlings were inoculated with either the transformants, the *pAVR3:GFP* recipient strain or water. Three weeks after inoculation disease development was assessed by scoring according to the disease index as described before (Rep *et al.*, 2004). Two out of three transformants lost their pathogenicity on susceptible C32 tomato plants (data not shown). The remaining transformant, however, showed a similar disease index as the Fol-*pAVR3:GFP* recipient strain on C32 tomato plants, showing that it is fully pathogenic (Figure 2A). In addition, both the original and the Avr2 replacement strain were unable to cause disease on *I-2* tomato plants, demonstrating that Avr2-RFP activates *I-2*-mediated resistance like wild-type Avr2 (Figure 2B). Collectively, these data demonstrate that the Avr2-RFP protein can complement Avr2 in both virulence and avirulence.

The complementing *Fol* p*AVR2*:*AVR2:RFP* transformant described above was used to study Avr2-RFP secretion and localization in tomato roots following inoculation on ten-day-old tomato seedlings. Based on the expression profile of *AVR2* determined above, roots were subjected to confocal microscopy starting at four days after inoculation. Clear RFP fluorescence was observed in distinct spots aligning the fungal hyphae growing in the cortical cells suggesting high local accumulation of Avr2 at an unknown structure (Figure 3A, arrows). No fluorescence was observed in the cytoplasm or nucleus of the host cells. A similar Avr2 localization pattern was found in transformants in which the p*AVR2*:*AVR2-RFP* gene had integrated at ectopic locations in the genome (Figure 3B, arrows). The relative low resolution of the image, likely caused by the thickness of the root tissue, prevented determination of the exact position of the spots relative to the fungal cell wall. Hence, we could not distinguish whether the spots are localised at a fungal-derived structure or inside the plant cell. To exclude the possibility that the red dots are caused by auto fluorescence from callose depositions or papilla outside of plant plasma membrane the Fol-p*AVR3:GFP* recipient was analysed for comparison. No red spots were observed for the control strain (Figure 3C), which demonstrates that the fluorescence of the spots is indeed caused by the Avr2-RFP fusion protein and not by fluorescent structures from the plant as a response to *Fol* infection. We therefore conclude that Avr2-RFP accumulates in spot-like structures, of unknown identity.

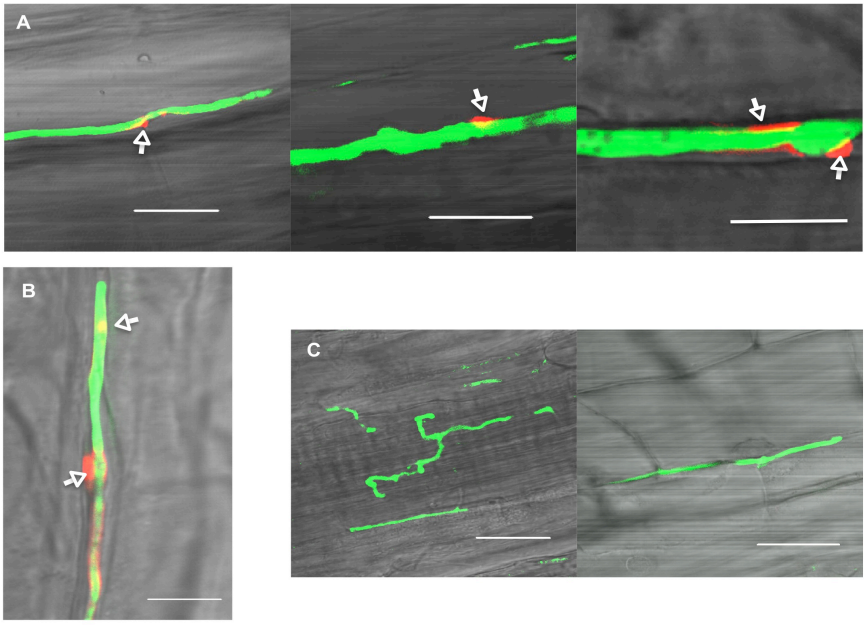

Figure 3. Localization of Avr2 upon *Fol* infection of tomato roots. RFP and GFP fluorescence was visualized using confocal imaging and is depicted in red and green, respectively. Ten-day-old tomato seedlings were inoculated with a spore suspension and four days after inoculation the roots were used for microscopical visualization. **A)** Transgenic *Fol* carrying both *AVR2:GFP,* whose expression is driven by the native *AVR2* promoter, and p*AVR3:GFP*. Arrows indicate the local accumulation of Avr2-RFP. **B)** Transgenic *Fol* carrying the ectopically integrated *AVR2:GFP* gene, but its expression is driven by the native *AVR2* promoter, and p*AVR3:GFP*. Arrows indicate the local accumulation of Avr2-RFP. **C)** *Fol* expressing only p*AVR3:GFP*. No RFP signal is detectable alongside the mycelium. White scale bars represent 50 µm.

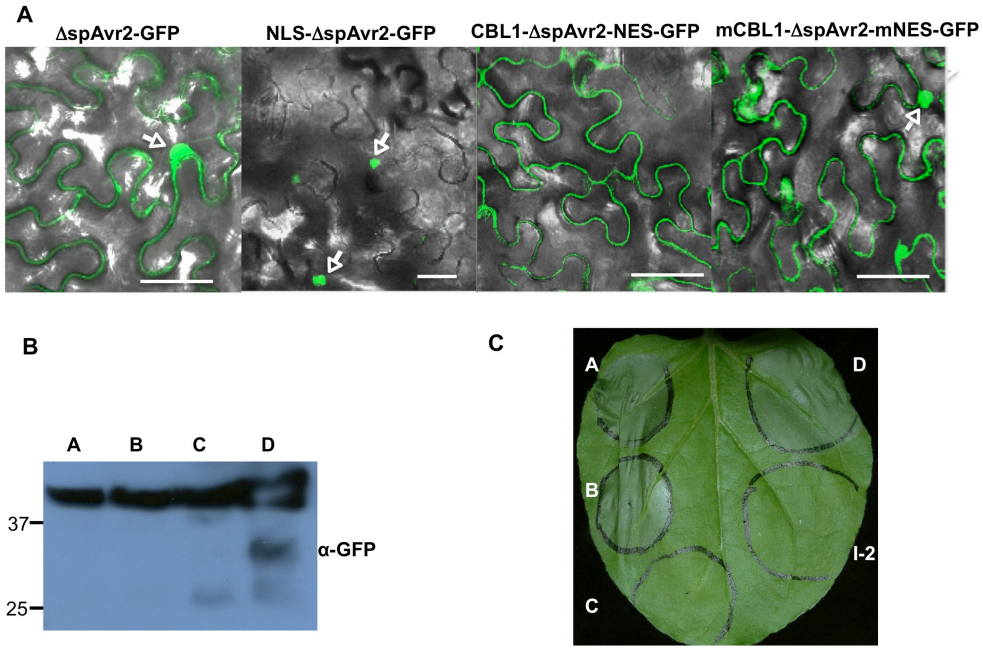

Figure 4. Nuclear localized Avr2 is required to trigger *I-2*-dependent cell death in *N. benthamiana* leaves. **A)** Confocal image of ΔspAvr2-GFP (A), NLS-ΔspAvr2-GFP (B), CBL1-ΔspAvr2-NES-GFP (C) and mCBL1-ΔspAvr2-mNES-GFP (D) in *N. benthamiana* leaves 36 h after agro-infiltration. The white scale bars represent 25 µm. **B)** Immunoblot analysis of GFP fusion proteins accumulating *in planta* 36 h after infiltration. Blots were probed with an α-GFP antibody. Sizes in kDa are indicated on the left. **C)** Nuclear localization is

required for effector-triggered cell death. *N. benthamiana* leaves co-infiltrated with Agrobacterium strains carrying ΔspAvr2:GFP (A), NLS-ΔspAvr2:GFP (B), CBL1-ΔspAvr2-NES:GFP (C) or mCBL1-ΔspAvr2-mNES:GFP (D) together with *I-2*, or with *I-2* alone as the negative control. A representative picture was taken three days after infiltration.

Nuclear localized Avr2 is required to trigger *I-2*-dependent cell death in *N. benthamiana*

The confocal studies did not confirm the presence of Avr2 in plant cells upon *Fol* infection. Yet, intracellularly localized Avr2 is able to activate *I-2* suggesting an intracellular localization. To determine the precise subcellular localization of this protein we employed a heterologous expression system. Thereto *AVR2* was expressed in *N. benthamiana* leaves using agroinfiltration. An advantage of this system is that the subcellular location of GFP-tagged Avr2 can be readily visualised in the transformed epidermal cells using confocal microscopy. When co-expressed with its cognate resistance gene *GFP-AVR2* is able to trigger *I-2*-dependent cell death, allowing us to link its subcellular location to its I-2 inducing activity (Chapters 3 and 6).

To determine at which subcellular localization Avr2 is able to trigger *I-2* mediated cell death, *AVR2* was fused either to a nuclear import signal (NLS) or to a CBL1 (Myristoylation signal) motif and a nuclear export signal (NES) at its N-terminus and C-terminus, respectively. A CBL1 motif tethers the Avr2 protein to the plasma membrane preventing intracellular diffusion and excluding it from entering the nucleus. As a negative control an Avr2 fusion with a mutated CBL1 (mCBL1) and NES (mNES) was made, resulting in the following three constructs: *NLS-*Δ*spAvr2:GFP*, *CBL1-*Δ*spAvr2-NES:GFP* and m*CBL1-*Δ*spAvr2-mNES:GFP*. To examine whether the localization signals are functional, the constructs were ectopically expressed in *N. benthamiana* leaves by agroinfiltration. At 36 h after infiltration, green fluorescence was imaged using confocal microscopy. As observed before, wild-type Avr2, lacking its signal peptide (Δsp) and fused to GFP, localized in both cytosol and nucleus (Figure 4A, arrow). NLS tagged Avr2-RFP (NLS-ΔspAvr2-GFP) was only detected in the nucleus and not in the cytoplasm (Figure 4A, arrows). In contrast, the CBL1 and NES tagged Avr2 (CBL1-ΔspAvr2-NES-GFP) protein was only found at the plasma membrane and not in the nucleus (Figure 4A). The Avr2 variant carrying the mutated CBL1 and NES signals (mCBL1-ΔspAvr2-mNES-GFP) displayed a similar distribution pattern as wild-type ΔspAvr2. Subsequently, we assessed the accumulation of the Avr2 variants by immunoblot analysis and detected the proteins using a GFP antibody. The immunoblot shows that all ΔspAvr2-GFP fusion proteins accumulate. The majority of the protein is intact as bands were found at the expected size of ~43 kDa, corresponding to that predicted for the full-length fusion protein. For the CBL1-Avr2-NES-GFP and mCBL1-Avr2-mNES-GFP extracts also some smaller bands were observed, which could be the consequence of limited proteolytic cleavage of the latter proteins (Figure 4B).

We next utilized the above described constructs to assess whether the forced localization of Avr2 affected its ability to trigger *I-2* mediated resistance. Thereto *I-2* and the three *AVR2* constructs carrying the various translocation signals were co-expressed in *N. benthamiana* leaves using agroinfiltration. Figure 4C shows that, at approximately 36 h after co-infiltration, nuclear localized NLS-ΔspAvr2-GFP triggered an *I-2*-dependent cell death response equivalent to that of wild-type Avr2. In contrast, CBL1-Avr2-NES-GFP, which is retained in the plasma membrane, was unable to activate *I-2* and induce cell death. Avr2 fused to the mutated (inactive) CBL1 and NES motifs triggered an *I-2* specific cell death response similar to that of the wild-type protein showing that the mere extension of Avr2 with these sequences did not interfere with its activity (Figure 4C). *I-2* alone was used as a negative control and as shown in figure 4C no cell death is induced in the infiltrated sector. In summary, these results indicate that a nuclear localization of Avr2 is required to trigger *I-2*-dependent cell death.

The N-terminal region of Avr2 is dispensable to trigger *I-2*-mediated cell death

To define the minimal region of Avr2 required to trigger *I-2*-dependent cell death, two N-terminally truncated and one C-terminally truncated Avr2 protein was generated. To assist demarcation of the Avr2 truncations, the secondary structure of Avr2 protein was predicted using PSIPRED (Buchan *et al.*, 2010) (Figure 5A). Based on the predicted structure, we constructed three variants: Avr2 Δ37, in which the first predicted random coil after signal peptide was deleted; Avr2 Δ40, in which the deletion extends till after the first cysteine; and Avr2 CTΔ11, which carries a deletion of the last β-sheet at its C-terminus (Figure 5B).

A. tumefaciens strains containing plasmids encoding these truncated *AVR2* constructs were co-infiltrated with an *A. tumefaciens* strain harbouring *I-2* into *N. benthamiana* leaves. Infiltration of the full-length Avr2 protein, lacking its signal peptide (Δsp), together with *I-2* served as a positive control. *I-2* alone was included as a negative control. Compared to the intact ΔspAvr2 protein, Avr2 Δ37 induced a much faster and stronger cell death response (Figure 5C). *I-2*-dependent cell death triggered by Avr2 Δ37 was observed as early as 20 to 24 h after infiltration, whereas cell death induced by wild-type Avr2 did not appear until 10 to 12 h later. Expression of the two other truncated variants: Avr2 Δ40 and CTΔ11 did not activate *I-2*-dependent cell death (Figure 5C).

Immunoblotting analysis demonstrated that all truncated proteins accumulated at similar levels, except for the Avr2 Δ37 truncation that accumulated in much higher amounts (Figure 5D). Hence, the inability of Avr2 Δ40 and CTΔ11 to trigger *I-2* mediated cell death is not due to a lack of protein accumulation. The high accumulation of Avr2 Δ37 might be correlated with its ability to trigger a faster and stronger cell death response. Based on these observations we concluded that Avr2 can be functionally divided into two parts, a small N-

terminal part that is not required for *I-2* mediated cell death and a C-terminal region that is indispensable for this activity.

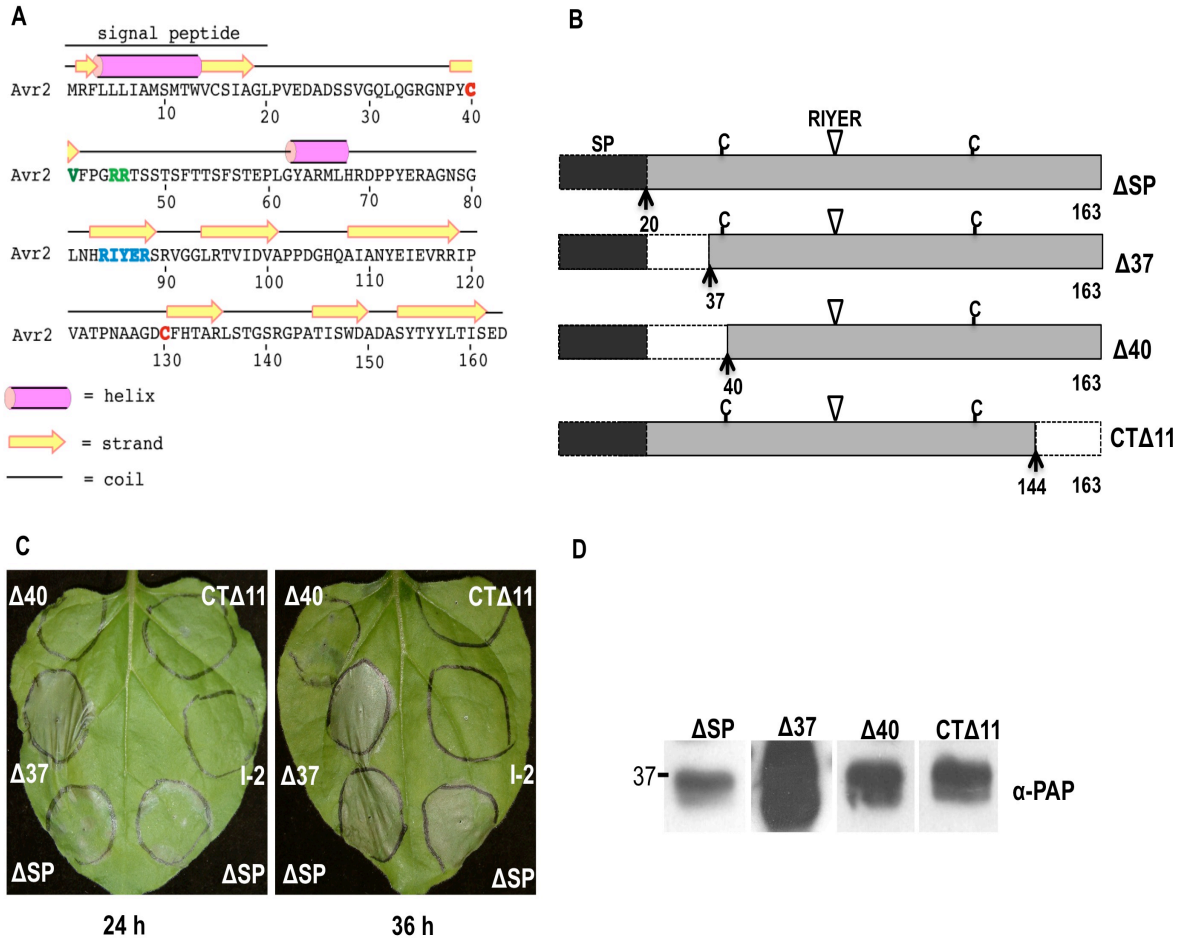

Figure 5. A small N-terminal region of Avr2 is dispensable for *I-2*-dependent cell death. **A)** Secondary structure prediction of the full length Avr2 protein. The two cysteine residues are marked red. The tree polymorphisms in *I-2* breaking Avr2 variants are marked green. The 'RIYER' motif is marked blue. **B)** Schematic diagram showing Avr2 truncations and their sizes. The signal peptide is shaded dark, the triangle indicates the position of the RIYER motif and C indicates a cysteine residue; N- and C-terminal truncation sites are indicated by dashed lines and arrows along with the corresponding amino acid number. **C)** *N. benthamiana* leaves were co-infiltrated with *Agrobacterium* cultures containing *AVR2* truncations and *I-2*. The left panel shows a leaf photographed 24 h after infiltration. The leaf in the right panel leave was photographed 36 h after infiltration. **D)** Immunoblot of protein extracts from agroinfiltrated *N. benthamiana* leaves transiently expressing Avr2 truncations fused C-terminally to a TAP tag. Leaves where harvested 36 h after infiltration and analyzed by immunoblotting using an anti-PAP antibody recognizing the TAP tag (α-PAP). Sizes in kDa are indicated on the left.

Mutation of the "RIYER" motif abolishes the function of Avr2

To assess the role of the "RIYER" motif for the function of Avr2 it was changed into QIVEQ. The same replacement was made in both wild-type Avr2 and a truncated version lacking the signal peptide. Both proteins were produced as C-terminal translational fusions to RFP. The localization of Avr2(riyer)-RFP and ΔspAvr2(riyer)-RFP was examined by

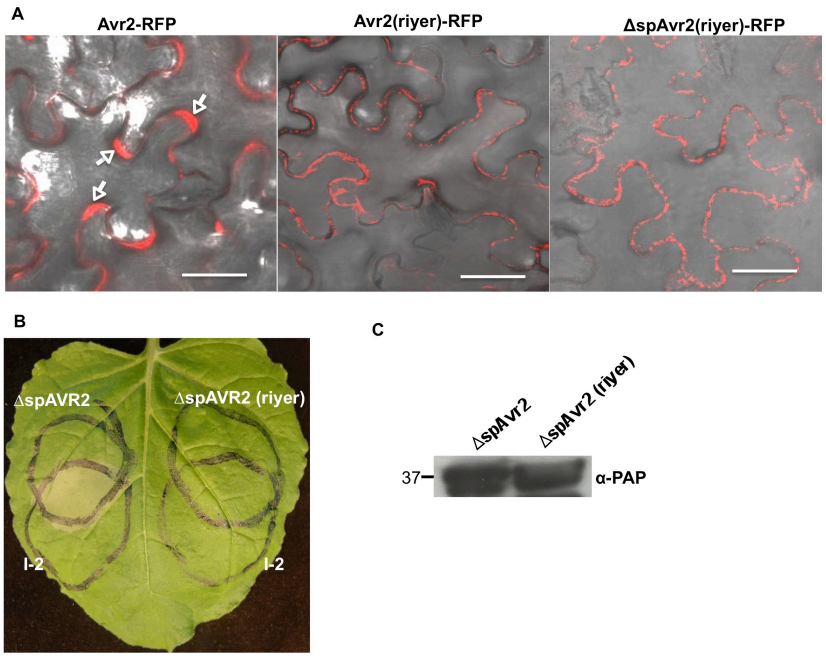

Figure 6. Mutations in the 'RIYER' motif abolish Avr2 secretion and recognition by I-2 function. A) Confocal images of mesophyll cells in *N. benthamiana* leaves 36 h after agro-infiltration with Avr2-RFP, Avr2(riyer)-RFP and ΔspAvr2(riyer)-RFP lacking its signal peptide for extracellular secretion. The white scale bars are 25 µm in length. White arrows indicate the apoplastic spaces. **B)** *N. benthamiana* leaves were agro-infiltrated with constructs containing *AVR2(riyer):RFP*, Δsp*AVR2(riyer):RFP* or *I-2*. The upper circles are infiltrated with *A. tumefaciens* carrying either a binary construct containing Δsp*AVR2:RFP* (left side of the leaf) or Δsp*AVR2(riyer):RFP* (right side of the leaf). The lower circles are I-2-infiltrated zones. Both genes are co-expressed at the overlapping zone. Representative leaves were photographed 3 days after infiltration. **C)** Protein extracts from agroinfiltrated *N. benthamiana* leaves transiently expressing Δsp*AVR2* and Δsp*AVR2(riyer)*. The encoded proteins are C-terminally fused to a TAP tag to allow their detection on an immunoblot using a α-PAP antibody. Sizes in kDa are indicated on the left.

confocal microscopy and compared to that of the wild-type Avr2-RFP protein. The red fluorescence originating from the wild-type Avr2-RFP fusion is mainly found in the apoplastic space, as indicated by arrows (Figure 6A). The dispersed RFP signal suggests that the protein is secreted in the apoplast and diffuses between the plant cells. Surprisingly, the accumulation of Avr2(riyer)-RFP and ΔspAvr2(riyer)-RFP differed very much from that of the wild-type protein and red fluorescence was mainly observed in large intracellular punctuate structures (Figure 6A). No RFP signal was detect in the apoplast for ΔspAvr2(riyer)-RFP nor for Avr2(riyer)-RFP despite the signal peptide in the latter protein. Next, the ability of the RIYER mutants to trigger *I-2*-mediated cell death was assessed. *A. tumefaciens* harbouring either the wild-type *AVR2:TAP* or the mutant Δsp*AVR2*(riyer):*TAP* construct was infiltrated in *N. benthamiana* leaves as overlapping circles with an *A. tumefaciens* strain carrying a plasmid encoding I-2. Figure 6B clearly shows that co-expression of wild-type Δsp*AVR2* and *I-2* resulted in cell death in the overlapping region. Cell death was not induced in the region where both Δsp*AVR2*(riyer):*TAP* and *I-2* were

expressed, suggesting that the mutation in the RIYER motif impaired the ability of Avr2 to activate I-2. Immunoblot analysis with anti-pap antibody confirmed expression and accumulation of both the wild-type ΔspAvr2-TAP and the ΔspAvr2(riyer)-TAP protein in infiltrated leaves (Figure 6C), showing that the absence of cell death was not caused by a reduced accumulation of the mutant protein but can be attributed to the mutation.

Avr2 homodimerizes *in vivo*

Immunobloting of agroinfiltrated *N. benthamiana* leaves expressing Avr2 equipped with an HASBP-tag, frequently revealed an additional of ~50 kDa band that has twice the molecular mass of the Avr2-HASBP protein of ~25 kDa (Figure 7). Since this larger product cross-reacted with the HA antibody it likely contains the Avr2-HASBP protein incorporated in a larger protein complex. To identify the proteins present in this complex a mass spectrometric analysis was performed. Avr2-HASBP containing complexes were purified with SBP beads

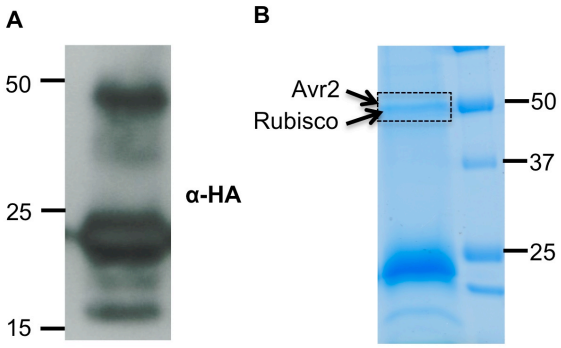

Figure 7. Avr2 is present in a high molecular weight complex. A) Immunoblot probed with anti-HA showing that Avr2 is detected at the expected apparent molecular weight of ±25kDA and as an ±50 kDa band. **B)** Avr2-HA-SBP was expressed in *Agrobacterium*-infiltrated *N. benthamiana* leaves and subsequently affinity-purified using the SBP tag. The purified protein was size separated using SDS-PAGE and the gel was stained with Colloidal Coomassie. The dashed rectangle indicates that the section was cut out for mass spectrometric analysis. Identified proteins in the sliced band are indicated on the left. Positions and sizes of protein molecular mass standards are shown.

from a total protein extract isolated from *N. benthamiana* leaves transiently expressing *AVR2-HASBP*. Next the Avr2 complexes were size-separated on SDS-PAGE and a region corresponding to the ~50 kDa product was cut out from the gel (Figure 7). The slice was used for in-gel digestion and subsequent mass spectrometric analysis. Besides Avr2 only Rubisco was identified in the peptide list. Since the latter is a likely contaminant the absence of other proteins raised the possibility that Avr2-HASBP might actually homodimerize giving rise to the 50 kDa product.

To assess a potential physical self-interaction of Avr2 *in planta*, we performed co-immunoprecipitation experiments. Thereto, two different *AVR2* constructs were made that both carry a different epitope tag: HASBP or GFP. Following agroinfiltration of these

constructs into *N. benthamiana* leaves one of the Avr2 proteins was pulled down using SBP affinity beads and co-purification of the other was assessed using its unique GFP tag. Figure 8A shows that GFP-tagged Avr2 co-precipitates with HASBP-tagged Avr2 when both genes were co-expressed in *N. benthamiana* leaves demonstrating that Avr2 has the ability to homodimerize.

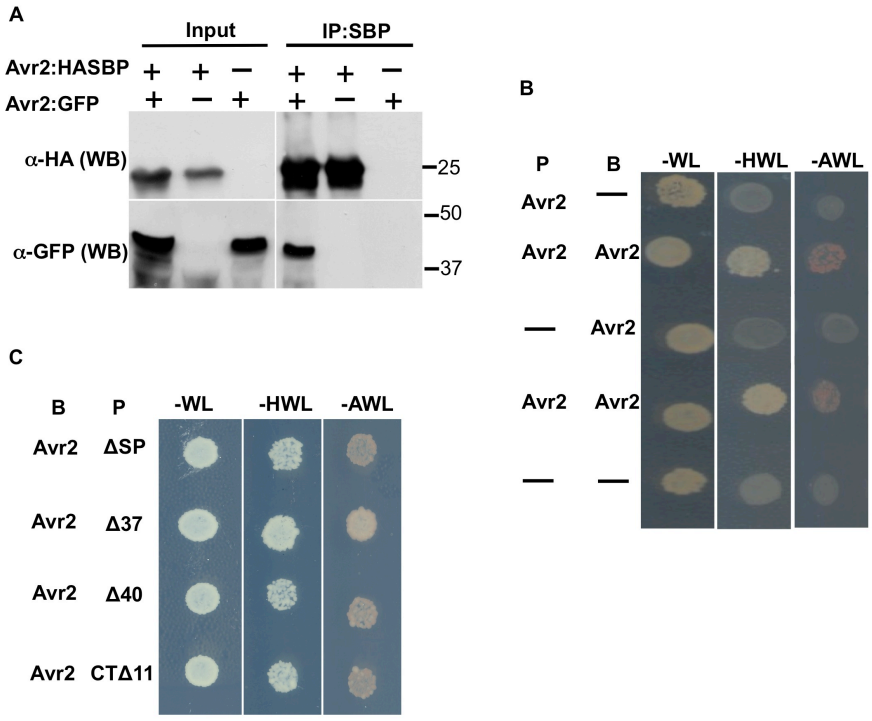

Figure 8. Avr2 forms homodimers *in planta* and in yeast. **A)** Immunoprecipitation of Avr2 from total plant protein extracts. Proteins extracted from *N. benthamiana* leaves expressing pairwise combinations of Avr2 C-terminal tagged with either an HASBP or a GFP tag. The fusion proteins were immunoprecipitated using streptavidin beads. Total extracted proteins (input) and immunoprecipitated proteins (IPs) were analysed by immunoblotting by probing with either anti-HA (α-HA; upper) or anti-GFP (α-GFP; lower). Positions and sizes of protein molecular mass standards are shown. **B)** Growth of yeast strain pJ694a transformed with prey (P) constructs containing *AVR2* or empty vector (-) and bait (B) constructs containing *AVR2* or empty vector (-). All transformed yeasts could grow on minimal media lacking tryptophan and leucine (-WL) due to presence of the bait and prey plasmids. Only yeast containing both Avr2 as prey and bait was able to grow on selection plates lacking histidine, tryptophan and leucine (-HWL) and the more stringent selection lacking alanine, tryptophan and leucine (-AWL). Neither empty bait or prey or Avr2 alone in combination with an empty vector could grow on the selection plates. **C)** All Avr2 truncations interacted with wild-type Avr2 in yeast. All transformed yeasts could grow on the minimal media lacking tryptophan and leucine (-WL).

To test whether Avr2 dimerization *in vivo* requires plant proteins a yeast-two hybrid experiment was conducted using Avr2 both as bait and prey. As shown in Figure 8B, Avr2 interacted with itself, as yeast transformed both with bait and prey plasmids harbouring Avr2 grew on the selective -HWL and also on the more stringent -AWL medium (Figure 8B). Yeast co-transformed with Avr2 and empty bait or prey plasmid was unable to grow on the selection plates (Figure 8B). Together, these data demonstrate that Avr2 can form dimers *in vivo*.

To determine whether Avr2 dimerization correlated with its avirulence activity we tested the three truncated Avr2 variants that we examined before for their ability to activate *I-2*-dependent cell death. Hereto we performed yeast two-hybrid assays using the Avr2 variants as preys and Avr2 wild-type as bait. Variant Avr2 Δ37, shown to be able to trigger *I-2*-dependent cell death (Figure 5), interacted with full length Avr2 as yeast transformed with both constructs grew on selective -HWL and -AWL medium (Figure 8C). Interestingly, the other two Avr2 truncations Avr2 Δ40 and Avr2 CTΔ11, both unable to activate *I-2*, were still able to interact with Avr2, as the transformed yeasts grew on the selection medium (Figure 8C). Together, these data show that other regions than the deleted parts in Avr2 are responsible for dimerization. Furthermore, sequences present in the deleted regions are important for avirulence, and dimerization of the remaining fragment is insufficient to induce *I-2*-mediated cell death.

Discussion

Expression of *AVR2* and localization of the protein *in planta*

Expression studies of *AVR3* (*SIX1*) revealed that this gene is expressed early upon *Fol* penetration of the tomato root cortex and it can be visualised already one-day post inoculation (Figure 1). The gene continues to be expressed during later stages of infection (van der Does *et al.*, 2008). Expression of *AVR2* in tomato roots infected with *Fol* was rarely observed during the early infection stages at one day after inoculation (Figure 1). However, *AVR2* expression was frequently seen in xylem-colonizing hyphae at four days after inoculation (Figure 1). Previous studies showed that expression of most *SIX* genes, including *AVR3* (*SIX1*) and *AVR2* (*SIX3*), depends on the presence of the transcription factor *SGE1* (SIX Genes Expression 1) (Michielse *et al.*, 2009). The delayed expression of *AVR2,* as compared to *AVR3,* indicates that expression of *AVR2* is not only regulated by *SGE1* but might be co-regulated by other factors. It will be interesting to analyse the expression profile of other *SIX* genes during infection and to compare these to those of *AVR3* and *AVR2* to identify whether they are controlled by similar or different regulatory elements. The relative late expression of *AVR2* suggests that *I-2* mediated resistance occurs relative late in infection when the fungus colonises the xylem vessels. This hypothesis is in agreement with i) the observed expression of *I-2* in the vasculature and its lack of expression in the cortical root cells and ii) the observation that in an *I-2* plant *Fol* colonises the cortical cells of the root and is able to reach the xylem vessels, but is confined in those vessels in an incompatible infection ((Mes *et al.*, 2000) and Martijn Rep, personal communication).

When determining the localization of the Avr2-RFP fusion protein during *Fol* infection, RFP fluorescence was only detected in small dots aligning hyphae growing between cortical cells (Figure 3A). These observations are based on the analysis of a single

in locus Avr2 transformant. However, in this transformant the *AVR2-RFP* transgene fully complemented both pathogenicity and *I-2* mediated resistance on tomato suggesting a functional effector protein (Figure 2). Furthermore, a similar Avr2 localization pattern was found in transformants in which the *AVR2-RFP* gene had integrated at ectopic locations in the genome (Figure 3B). Because of the limited resolution of the images, we cannot determine the exact localization of these spots in relation to the fungal or plant cell walls. The lack of discernible RFP signals in the host cells and xylem vessels may be due to rapid diffusion of the Avr2-RFP protein leading to fluorescent signals that are below our detection limits. Such an explanation corresponds with observations made in translocation studies of fluorescent-labelled effectors from other pathogens such as the RXLR effectors from oomycetes or effectors from *Colletotrichum higginsianum* (Kleemann *et al.*, 2012; Whisson *et al.*, 2007). In these studies, fluorescently labelled effector proteins could also not been visualised intracellularly in infected host cells. To our knowledge, so far only the *Magnaporthe oryzae* effector PWL2 labelled with RFP could be visualised in infected host cells by increasing the pinhole diameter of confocal microscopy to allow detection of the very weak fluorescent signals (Khang *et al.*, 2010). However, in our study an increased pinhole diameter increased the red auto-fluorescent background of the roots making it impossible to distinguish between the RFP signal and the background. An alternative explanation for the lack of a cytoplasmic RFP signal in the tomato cells would be proteolytic cleavage of the RFP tag in the xylem sap. Such a cleavage event could leave a non-fluorescent, but intact and functional Avr2 protein that could be taken up by the host cell. Similar cleavage is found when apoplastically localised Avr2 is produced in *N. benthamiana* leaves upon agroinfiltration (data not shown). Using a RFP antibody immunoblotting analysis of xylem sap from AVR2-RFP *Fol* infected tomato plants could reveal whether similar cleavage occurs in the xylem sap. Collectively, our localization studies revealed a novel structure in which the Avr2 protein accumulates. It will be interesting to establish the identity of this structure and to test whether it is also targeted by other *Fol* effectors as this identity could provide insight in the function of Avr2. If the RFP protein is proteolyticly cleaved from Avr2 in the xylem sap than alternative approaches such as immunolocalization are required to show its location inside host cells.

Although RFP labelled Avr2 could not be observed intracellularly during *Fol* infection (Figure 3), *in vitro* entry assays performed by Kale and coworkers demonstrated that truncated Avr2, heterologously produced in *E.coli,* is able to enter soybean root cells (Kale *et al.*, 2010). The authors reported that entry of Avr2 into plant cells require an intact RxLR-like motif as mutation of the “RIYER” motif in Avr2 abolished entry into plant cells (Kale *et al.*, 2010). This observation supports the translocation mechanism they have proposed for oomycete RxLR effectors and fungal effectors carrying RxLR-like motifs. In this model RxLR or RxLR-like motifs enable the effector to bind phosphatidylinositol 3-

phosphate (PI3P) present on the outer surface of the plant plasma membrane. Binding to these lipids is anticipated to trigger an endocytotic process mediating effector uptake into the plant cells (Kale *et al.*, 2010). The RxLR-like RIYER sequence is located in the middle of Avr2 (Figure 5A). Our findings revealed that mutation of the RIYER sequence resulted in an Avr2 protein that is prone to aggregation and could be no longer secreted when transiently expressed in plant cells (Figure 6A). Furthermore, the mutated Avr2 protein was impaired in its ability to trigger *I-2*-dependent cell death (Figure 6B). Together, these observations suggest that the RIYER motif has an important structural role in folding/stabilizing Avr2 and the reported lack of uptake and lipid binding could be explained by an improper protein fold rather than reflecting an intrinsic property of the RIYER motif. Since truncated Avr2 was used for the uptake assays and PI3P binding assays performed by Kale and coworkers, it will be very interesting to determine whether full length Avr2 protein behaves the same in these assays.

The role of nuclear localized Avr2 in *I-2*-mediated cell death

Intracellular localized Avr2 is able to activate I-2 when transiently produced in *N. benthamiana* leaves (Chapter 6). Using the same expression system, we here demonstrate that actually a nuclear localization for Avr2 is required to trigger an *I-2*-dependent cell death response (Figure 4). Unfortunately, the subcellular localization of I-2 is unknown and its determination is hampered by the lack of sensitive antibodies and the observed loss-of-function of tagged I-2 variants (Tameling *et al.*, 2002). A truncated I-2 protein, lacking its LRR domain, was found to localize in both the nucleus and the cytosol when expressed via agroinfiltration in *N. benthamiana* (data not shown). In addition, a potential nuclear localization signal (RKHK) has been predicted in the CC domain of I-2 (Simons *et al.*, 1998). These observations imply that I-2 could be localized in the nucleus, which would result in a co-localization of Avr2 and I-2 in the nucleus. A growing body of evidence suggest that nuclear or a nucleocytoplasmic localization of R proteins is essential for plant immune signalling (Deslandes and Rivas, 2011; Rivas, 2012). For instance, the *P. syringae* effector AvrRps4 was found to trigger compartment-specific immune responses in which nuclear localized AvrRps4 triggers RPS4-dependent resistance and cytoplasmic AvrRps4 induces cell death, implying that cell death and resistance signalling are branched processes (Heidrich *et al.*, 2011). Also the barley resistance protein MLA10 displays compartment-specific immunity; the nuclear pool being involved in resistance and the cytoplasmic pool in triggering cell death. These observations suggest that effective immune responses require coordination of different compartment-specific immune response (Bai *et al.*, 2012). It will be interesting to determine whether Avr2-mediated cell death and resistance also branch into specific subcellular compartments or whether both coincide within the plant nucleus.

Structure-function analysis of Avr2

Deletion studies based on the predicted secondary structure of Avr2 (Figure 5A) showed that the N-terminal 17 amino acids (Δ37) following the signal peptide are not required to trigger *I-2*-dependent cell death. This finding is consistent with our proteomic data obtained from analyses of xylem sap from infected tomato plants. On 2D gels Avr2 was found in at least three spots ranging in size from 11 to 14 kDa. Their peptide mass spectra showed that the smallest form of Avr2 has a N-terminal deletion similar to that of Δ37 (Houterman *et al.*, 2007). The mechanisms behind of removal of these 17 aa is unknown, but might be due to N-terminal processing by plant proteases. Although full length Avr2 is able to homodimerize in yeast and *in planta* (Figure 8A and B), these extra 17 amino acids are not required for homodimerization. Actually, upon agrotransformation the truncated protein induced a faster and stronger cell death response than that of a full length Avr2 protein, which correlated with an increased accumulation of the truncated protein. (Figure 5C). The mechanism underlying the higher accumulation of this truncated protein is unknown.

An extended deletion removing 20 amino acids at the N-terminus encompassing the first cysteine after the signal peptide (Δ40) completely abolished the ability of Avr2 to trigger *I-2*-dependent cell death (Figure 5C). Since there are two cysteine residues present in Avr2 (Figure 5A), it is tempting to speculate that a disulfide bond is formed in the mature Avr2 protein. Deletion of the cysteine would disrupt this bond potentially affecting protein structure. However, the protein apparently retains at least part of its fold, as the mutant is still able to interact with wild-type Avr2 in yeast. Likewise, a C-terminal deletion abolished *I-2* mediated recognition but retained the proteins' ability to interact with wild-type Avr2 in yeast (Figure 8C). These data show that the core of Avr2, which is required for dimerization, is insufficient to activate I-2 suggesting that the C-terminus contains sequences required for recognition (Figure 8C). To fully understand the underlying mechanism elucidation of the 3D protein structure of Avr2 is required. Having the structure will aid identification of surface residues required for homodimerization, and the interaction with plant proteins, such as I-2.

Materials and methods

Plant materials and fungal isolates

The tomato (*Solanum lycopersicum*) cultivars used in this study are C32, which is susceptible to *Fol* (Kroon and Elgersma, 1993), and 90E341F (Stall and Walter, 1965), which is resistant to Race 2. A *Fusarium oxysporum* f.sp. *lycopersici* strain 007 (Fol007) in which the *AVR3* gene has been replaced by *GFP* was used as recipient strain for fungal transformations (Houterman *et al.*, 2009; van der Does *et al.*, 2008). All of the *Fol* strains used are listed in Table S1.

Plant inoculations

Fol was grown in minimal medium (100 mM KNO_3, 3% sucrose and 0.17% Yeast Nitrogen Base without amino acids or ammonia) and spores were harvested after three-five days of cultivation at 25

ºC with shaking. After washing with sterilized water the spores were diluted to 10^7 spore/ml. For bioassays ten-day-old tomato seedlings were used according to the root dip method (Mes *et al.*, 1999). For microscopical analyses ten-day-old tomato seedlings were taken carefully from soil and their roots were washed gently with tap water. After washing, the seedlings were placed into a Petri dish prefilled with 25 ml spore suspension. The seedlings where leaning against the side of the petridish and their roots where spread out evenly. At various time-points after co-cultivation the roots were examined using confocal microscopy.

Generation of transgenic *Fol* strains

Homologous recombination was used to replace the *AVR2* gene with a cassette containing the gene of interest and a hygromycin resistance gene. To generate *AVR2*-promoter-*RFP* and *AVR2*-promoter-*AVR2:RFP* constructs, the terminator of *AVR2* gene was PCR amplified with primer combination FP2708/FP2663 using Fol007 genomic DNA as template. The resulting amplicon was cloned into the *Kpn*I site of pRW2h:Δ*AVR2*. In this vector the hygromycin resistance gene cassette is flanked by 1266 bp and 717 bp of sequences upstream and downstream of the *AVR2* ORF (Houterman *et al.*, 2009). The correct orientation of the *AVR2* terminator was confirmed by PCR using primer set FP1074/FP2663. To construct the *AVR2*:*RFP* fusion fragment, overlap extension PCR was performed. The complete coding sequence of *AVR2* was amplified from Fol007 genomic DNA with primer combination FP2074/FP2665. Meanwhile, RFP was amplified from the pGWB454 plasmid DNA using primer set FP2666/FP2707 listed in Table S2 (Nakagawa *et al.*, 2007). The obtained PCR products were combined and used as templates for overlap extension PCR with primer set FP2704/FP2665. This 2nd PCR reaction resulted in the desired *AVR2:RFP* fusion fragment. To generate a *RFP* fragment flanked with *Spe*I sites, PCR was conducted using primer set FP2706/FP2707 with the pGWB454 plasmid as template. The obtained fragments were digested with *Spe*I, gel purified, and ligated into a *Spe*I digested pRW2h:Δ*AVR2*-T vector containing the *AVR2* terminator. The orientation of *AVR2:RFP* and *RFP* constructs was confirmed by PCR with primer set FP1074/FP2707. The obtained plasmids, either pRW2h:*pAVR2:RFP* or pRW2h:*pAVR2-AVR2:RFP,* were transformed into *Agrobacterium* EHA105 and used for subsequent Agrobacterium tumefaciens-mediated *Fol* transformation according to Rep *et al.*. (Rep *et al.*, 2004). Fol transformants capable of growing on 100 μg mL^{-1} hygromycin (Duchefa) were checked by PCR for the absence of the *AVR2* gene using primer pair FP1074/FP965. Presence of the right and left borders of these constructs was confirmed with primers annealing just outside the flanking sequences, these were FP745/FP1075 (right border) and FP659/FP1166 (left border), respectively.

Vector construction

For localization studies, the pENTR207:Δ*AVR2* plasmid, described previously (Houterman *et al.*, 2009), was used to recombine *AVR2* into binary vector pGWB451 (Nakagawa *et al.*, 2007) according to the Gateway protocol for LR recombination reaction (Invitrogen). In this construct pGWB451: Δ*AVR2* Avr2 is fused to a GFP tag present in the vector. To construct *NLS*-Δ*AVR2*:*GFP,* a nuclear localization signal (NLS) was introduced into forward primer FP2959 and the fragment was amplified together with reverse primer FP2222 from the pGWB451:Δ*AVR2* plasmid . To create *CBL*-Δ*AVR2*-*NES:GFP*, first a part of the myristolylation signal (CBL) (Batistic *et al.*, 2008) was introduced into forward primer FP3479 and part of the nuclear export signal was introduced into the reverse primer FP3483. The fragment obtained with this primer set was than used as template for a second round of PCR using primer set FP3478/FP3482. The resulted fragment contained the

complete CBL coding sequences in the N-terminus and a NES coding sequence in the C-terminus of *AVR2*. The fragment harbouring the mutated CBL and NES coding sequences was generated using the same strategy but by using primer sets FP3481/FP3485 and FP3480/FP3484, respectively. Finally the three amplicons were digested with *Xba*I and *Sac*I, and ligated into pGWB451 digested with the same enzymes.

Three primer combinations: FP2684/FP1751, FP2699/FP1751 and FP1749/FP2685 were used to amplify truncated *AVR2* fragments from CTAPi: Δ*AVR2*. Subsequently, gateway *attB* linkers were added via PCR using primers FP872 and FP873. The obtained PCR products were introduced into entry clone pDONR207 (Invitrogen, http://www.invitrogen.com/) using the Gateway protocol described by the manufacturer (Invitrogen). The hence obtained pENTR207::*ΔspAVR2*-Δ29 (N-terminal deletion-1), pENTR207::*ΔspAVR2*-Δ31 and pENTR207::*ΔspAVR2*-CTΔ11 (C-terminal deletion) plasmids were recombined into the binary vector CTAPi (Rohila *et al.*, 2004) using the Gateway protocol (Invitrogen). The resulting plasmids, CTAPi::*ΔspAVR2*-Δ29, CTAPi::*ΔspAVR2*-Δ31 and CTAPi::*ΔspAVR2*-CTΔ11, were used for Agro-transformation as described below.

To generate the constructs used for yeast-two hybrid experiments, the *AVR2* ORF*,* lacking the sequence encoding the signal peptide, was amplified using primer FP1873 and FP1874. As template the *AVR2* gene in CTAPi was used (Houterman *et al.*, 2009). The obtained product, carrying *Nco*I and *Eco*RI restriction sites, was cloned into the pAS2-1 and pACT-2 (Clontech) vectors digested with the same restriction enzymes.

For co-immunoprecipication experiments binary vectors containing Avr2 were created. *Xba*I and *Bam*HI restriction sites flanking the Δsp*AVR2* coding sequence were introduced by PCR with primers FP2525 and FP2274 using CTAPi*::*Δsp*AVR2* as template (Houterman *et al.*, 2009). The obtained product was sub-cloned into the vector SLDB3104 (Tameling *et al.*, 2010) between the *Xba*I and *Bam*HI restriction sites to generate SLDB3104::Δsp*AVR2*. In the resulting plasmid Avr2 is fused to a C-terminal HA and streptavidin-binding peptide (SBP) tag. All PCR primers were purchased from MWG (http://www.mwg-biotech.com), and sequences of all plasmids were confirmed by sequence analysis.

Protein extraction and immnuoblotting

Infiltrated *N. benthamiana* leaves were harvested and pooled 24 h after agro-infiltration, and subsequently snap-frozen in liquid nitrogen. After grinding the tissue with a mortar and pestle, it was allowed to thaw in 2 ml protein extraction buffer per gram of tissue [25 mM Tris pH 8, 1 mM EDTA, 150 mM NaCl, 5 mM DTT, 0.1% NP-40, 1× Roche complete protease inhibitor cocktail (http://www.roche.com) and 2% PVPP]. Extracts were centrifuged at 12 000 ***g,*** 4 °C for 10 min, and the supernatant was passed over four layers of Miracloth (http://www.calbiochem.com/miracloth) to obtain a total protein lysate. 40 μL samples were mixed with Laemmli sample buffer, and equal amounts of total protein were run on 13% SDS–PAGE gels and blotted on PVDF membranes using semi-dry blotting. Skimmed milk powder (5%) was used as a blocking agent. A 1:3000 dilution of anti-GFP antibody (VXA6455, Invitrogen), or 1:8000 dilution of anti-TAP tag antibody (PAP, P1291, Sigma P1291) linked to horseradish peroxidase were used. The secondary antibody goat-anti-rabbit (P31430, Pierce) was used as a 1:5000 dilution. The luminescent signal was visualized by ECL using BioMax MR film (Kodak, http://www.kodak.com).

For mass spectrometry analysis, protein extracts were spun for 10 min at 12,000g, and 1 mL supernatant was added to 100 µl bed volume of Streptavidin Sepharose High Performance beads (GE Healthcare). Protein extracts were incubated in a rotator for 3 h at 4°C, and washed four times with immunoprecipitation buffer (25 mM Tris-HCl, pH 7.5, 1 mM EDTA, 150 mM NaCl, 10% glycerol, and 5 mM DTT, and 0.15% Nonidet P-40). Elution was performed twice with two bed volumes of washing buffer containing 4 mM D-biotin (Sigma-Aldrich). 400 µl eluted fractions were pooled and precipitated with trichloroacetic acid. Pellets were washed with 100% acetone at -20 °C. 40 µl samples were mixed with Laemmli sample buffer for MS and loaded on 12% SDS-PAGE gels cased in Hoefer Might Small SE250 minigel equipment (Amersham Biosciences, AB, Uppsala). After gel electrophoreses Coomassie PageBlue™ (Fermentas) was used to visualize the proteins.

Mass spectrometry

The protein bands corresponding to the mass of the expected Avr2 monomer and dimer were sliced from the Coomassie stained gel. In-gel digestion was performed as described by Rep et al.. (Rep *et al.*, 2002). The peptides obtained after the digestion were analysed by MALDI-TOF/TOF MS as described by Krasikov et al. (Krasikov *et al.*, 2011). Acquired spectra were then searched with Mascot (Matrix Science, UK) against a *Fol* database. The *Fol* protein database used for the analysis was obtained from Fusarium Comparative Genome website (http://www.broadinstitute.org/annotation/genome/fusarium_group/MultiHome.html) and supplemented by adding the sequences of known SIX proteins that are not annotated in the public database. To identify the plant proteins, all spectra were also searched against a custom Solanaceae EST database from plant-assembled transcripts (http://plantta.jcvi.org/).

Yeast two-hybrid

The matchmaker GAL4 two-hybrid system and yeast strain PJ694a were used for analyzing protein interactions. Yeast transformation was performed using lithium-acetate and polyethylene glycol 3350 as described (Gietz and Woods, 2002). Eight colonies were picked and transferred from the MM-WL plates, lacking Trp and Leu, to a fresh MM-WL plate and incubated for 5 days at 30°C. Next, one colony per combination was re-suspended in 25 µl 0.9 % NaCl and 6 µl was spotted on MM-WL, MM-HWL, MM-AWL, and MM-HWL plates containing 3 mM 3-amino-1,2,4-triazole. After 5 days incubation at 30 °C, the plates were checked for growth and photographed.

Co-immunoprecipication

For Co-IP experiments, total proteins were extracted from *N. benthamiana* leaves, as described above, 36 h after infiltrating with *A. tumefaciens* GV3101 containing either SLD::Δsp*AVR2*-HASBP or pGWB451::Δsp*AVR2* or a mixture of both *A. tumefaciens* strains. Immunoprecipication was performed as described above. A portion of the supernatant was reserved as input sample. 20 µl immunoprecipicated samples and 40 µl input samples were resuspended in 1x SDS-PAGE loading buffer and loaded on 12% SDS-PAGE gels. Next, the gels were subjected to immunoblotting using anti-HA peroxidase at dilution ratio 1:3000 (clone 3F10; Roche), and anti-GFP at dilution ratio 1:3000 (Invitrogen, VXA6455).

Confocal microscopy

Confocal microscopical analysis was performed with the LSM510 (Zeiss, Germany). Excitation of the GFP was done at 488 nm with an Ar-ion laser and emission was captured with a 505-530 nm pass

filter. Excitation of the RFP occurred at 543 nm with a HeNe laser. The 590-620 nm filter captured emission. To monitor co-localization RFP was excited at 543 nm and GFP at 488 nm. GFP emission was captured with a 505-530 nm filter and RFP with a 565-615 nm filter. Images were scanned 8 times.

Agrobacterium*-mediated transient transformation of *Nicotiana benthamiana

Agrobacterium tumefaciens strain GV3101(pMP90) (Koncz and Schell, 1986) was transformed with binary constructs as described previously (Takken *et al.*, 2004). Agrobacterium-mediated transient transformation was performed according to methods described by Ma et al.. (Ma *et al.*, 2012). Briefly, the agrobacteria were grown to an absorbance of 0.8 at 600 nm in LB-mannitol medium (10 g l^{-1} tryptone, 5 g l^{-1} yeast extract, 2.5 g l^{-1} NaCl, 10 g l^{-1} mannitol) supplemented with 20 µm acetosyringone and 10 mm MES pH 5.6. Cells were pelleted by centrifugation at 4000 *g* at 20°C for 20 min and then resuspended in infiltration medium (1× MS salts, 10 mm MES pH 5.6, 2% w/v sucrose, 200 µm acetosyringone). Infiltration was done in *N. benthamiana* leaves at an absorbance of 0.1 (for *I-2* constructs) or 0.5 (for *AVR2* constructs) of 4–5-week-old plants.

Supplementary data

Table S1. *Fol* strains used in this study

Strains	Race	Transformed constructs
Fol007	2	Wild-type
Fol007(p*AVR3:GFP*)	2	*AVR3*-promoter-*GFP* (van der Does *et al.*, 2008)
Fol007(p*AVR3:GFP*+p*AVR2:RFP*)	2	*AVR3*-promoter-*GFP* and *AVR2*-promoter-*RFP*
Fol007(p*AVR3:GFP*+p*AVR2:AVR2-GFP*)	2	*AVR3*-promoter-*GFP* and *AVR2*-promoter-*AVR2:RFP*

Table S2. Primers used in this study

Number	Sequences
FP2708	GCGGTACCACTAGTTTCTGTGGCAGTTCCCCT
FP2663	CCCGGTACCCAGTCCCCACACAGTATTCTTTC
FP1074	CCAGCCAGAAGGCCAGTTT
FP2074	CGCACTAGTATGCGTTTCCTTCTGCTTA
FP2665	CGGAGGAGGCCATAGATCTATCCTCTGAGATA
FP2666	TATCTCAGAGGATAGATCTATGGCCTCCTCCG
FP2707	CGACTAGTAGATCTTTAGGCGCCGGTGGAGTGGCGG
FP2706	CCACTAGTATGGCCTCCTCCGAGGAC
FP2959	CCTCTAGATTGCTCACCTAAGAAGAGAAAGGTTGGAGGAC
FP2222	CGCGCGAGCTCTTATTTGTATAGTTCATCCA
FP3479	GCGTCTAGAATGGGCTGCTTCCACTCAAAGCAGCAAAAGAATTT
FP3483	GCGTCTAGAAAGAGTAAGTCTTTCAAGAGGAGGAAGTTGAAGATC
FP2704	CCACTAGTATGCGTTTCCTTCTGCTT

FP3818	CGACTAGTTTAAACCTTTCTCTTCTTCTTA
FP3819	CGACTAGTTTAAAGAGATAGTCTTTCAAGAGGA
FP3820	CAACTAGTTAAAACGGCTCTGGCAACGGCAGG
FP1749	AAAAAGCAGGCTGGATGCCTGTGGAAGATGCCGATTCATC
FP1751	AGAAAGCTGGGTATCCATC CTCTGAGATAGTAAGATAG
FP2684	AAAAAGCAGGCTCTATGCCATATTGCGTGTTTCCCGGCCG
FP2699	AAAAAGCAGGCTCTATGGTGTTTCCCGGCCGCCGCACG
FP2685	AGAAAGCTGGGTAAGCGTCGGCATCCCAACTGATTGTG
FP1074	CCAGCCAGAAGGCCAGTTT
FP965	CCACTGACTTGCCTAAAGC
FP1166	TAGCCTATTTGGAGTTCAGC
FP659	TAGAGATCATGCTATATCTC
FP745	GCATGTTTCTTCCTTGAACTCTC
FP1075	ACACACCAATTCACATCAATG

Acknowledgement

We are gratefully to Harold Lemereis, Ludek Tikovsky and Thijs Hendrix for taking care of the plant.

References

Alfano JR (2009) Roadmap for future research on plant pathogen effectors. *Mol Plant Pathol* **10:** 805-813.

armstrong GM, Armstrong JK (1981) *Formae speciales* and races of *Fusarium oxysporum* causing wilt diseases., University Park: PA: Penn State University Press.

Bai S, Liu J, Chang C, Zhang L, Maekawa T, Wang Q, Xiao W, Liu Y, Chai J, Takken FWL, Schulze-Lefert P, Shen Q-H (2012) Structure-function analyses of barley NLR immune receptor MLA10 reveal its subcellular specific activity in cell death signaling and disease resistance. *PLoS Pathog* **in press**

Batistic O, Sorek N, Schultke S, Yalovsky S, Kudla J (2008) Dual fatty acyl modification determines the localization and plasma membrane targeting of CBL/CIPK Ca2+ signaling complexes in Arabidopsis. *Plant Cell* **20:** 1346-1362.

Beckman CH (2000) Phenolic-storing cells: keys to programmed cell death and periderm formation in wilt disease resistance and in general defence responses in plants? *Physiol Mol Plant P* **57:** 101-110.

Buchan DWA, Ward SM, Lobley AE, Nugent TCO, Bryson K, Jones DT (2010) Protein annotation and modelling servers at University College London. *Nucleic Acids Res* **38:** W563-W568.

Chisholm ST, Coaker G, Day B, Staskawicz BJ (2006) Host-microbe interactions: Shaping the evolution of the plant immune response. *Cell* **124:** 803-814.

Deslandes L, Rivas S (2011) The plant cell nucleus: a true arena for the fight between plants and pathogens. *Plant Signal Behav* **6:** 42-48.

Di Pietro A, Madrid MP, Caracuel Z, Delgado-Jarana J, Roncero MIG (2003) *Fusarium oxysporum*: exploring the molecular arsenal of a vascular wilt fungus. *Mol Plant Pathol* **4:** 315-325.

Ellis JG, Rafiqi M, Gan P, Chakrabarti A, Dodds PN (2009) Recent progress in discovery and functional analysis of effector proteins of fungal and oomycete plant pathogens. *Curr Opin Plant Biol* **12:** 399-405.

Fisher MC, Henk DA, Briggs CJ, Brownstein JS, Madoff LC, McCraw SL, Gurr SJ (2012) Emerging fungal threats to animal, plant and ecosystem health. *Nature* **484:** 186-194.

Flor H (1942) Inheritance of pathogenicity in a cross between physiologic races 22 and 24 of *Melampsora lini*. *Phytopathology* **32:** 653-659.

Gassmann W, Bhattacharjee S (2012) Effector-triggered immunity signaling: from gene-for-gene pathways to protein-protein interaction networks. *Mol Plant Microbe Interact* **25:** 862-868.

Gietz RD, Woods RA (2002) Transformation of yeast by lithium acetate/single-stranded carrier DNA/polyethylene glycol method. *Methods Enzymol* **350:** 87-96.

Heidrich K, Wirthmueller L, Tasset C, Pouzet C, Deslandes L, Parker JE (2011) Arabidopsis EDS1 connects pathogen effector recognition to cell compartment-specific immune responses. *Science* **334:** 1401-1404.

Houterman PM, Ma L, van Ooijen G, de Vroomen MJ, Cornelissen BJC, Takken FLW, Rep M (2009) The effector protein Avr2 of the xylem-colonizing fungus *Fusarium oxysporum* activates the tomato resistance protein I-2 intracellularly. *Plant J* **58:** 970-978.

Houterman PM, Speijer D, Dekker HL, de Koster CG, Cornelissen BJC, Rep M (2007) The mixed xylem sap proteome of Fusarium oxysporum-infected tomato plants. *Mol Plant Pathol* **8:** 215-221.

Jones JD, Dangl JL (2006) The plant immune system. *Nature* **444:** 323-329.

Kale SD, Gu B, Capelluto DG, Dou D, Feldman E, Rumore A, Arredondo FD, Hanlon R, Fudal I, Rouxel T, Lawrence CB, Shan W, Tyler BM (2010) External lipid PI3P mediates entry of eukaryotic pathogen effectors into plant and animal host cells. *Cell* **142:** 284-295.

Kamoun S (2006) A catalogue of the effector secretome of plant pathogenic oomycetes. *Annu Rev Phytopathol* **44:** 41-60.

Khang CH, Berruyer R, Giraldo MC, Kankanala P, Park SY, Czymmek K, Kang S, Valent B (2010) Translocation of *Magnaporthe oryzae* effectors into rice cells and their subsequent cell-to-cell movement. *Plant Cell* **22:** 1388-1403.

Kleemann J, Rincon-Rivera LJ, Takahara H, Neumann U, van Themaat EV, van der Does HC, Hacquard S, Stuber K, Will I, Schmalenbach W, Schmelzer E, O'Connell RJ (2012) Sequential delivery of host-induced virulence effectors by appressoria and intracellular hyphae of the phytopathogen *Colletotrichum higginsianum*. *PLoS Pathog* **8:** e1002643.

Koeck M, Hardham AR, Dodds PN (2011) The role of effectors of biotrophic and hemibiotrophic fungi in infection. *Cell Microbiol* **13:** 1849-1857.

Koncz C, Schell J (1986) The Promoter of Tl-DNA gene 5 controls the tissue-specific expression of chimeric genes carried by a novel type of Agrobacterium binary vector. *Mol Gen Genet* **204:** 383-396.

Krasikov V, Dekker HL, Rep M, Takken FLW (2011) The tomato xylem sap protein XSP10 is required for full susceptibility to Fusarium wilt disease. *J Exp Bot* **62:** 963-973.

Kroon BAM, Elgersma DM (1993) Interactions between Race-2 of *Fusarium oxysporum* f. sp. *Lycopersici* and near-isogenic resistant and susceptible lines of intact plants or callus of Tomato. *J Phytopathol* **137:** 1-9.

Lukasik E, Takken FLW (2009) STANDing strong, resistance proteins instigators of plant defence. *Curr Opin Plant Biol* **12:** 427-436.

Ma L, Lukasik E, Gawehns F, Takken FL (2012) The use of agroinfiltration for transient expression of plant resistance and fungal effector proteins in *Nicotiana benthamiana* leaves. *Methods Mol Biol* **835:** 61-74.

Maekawa T, Kufer TA, Schulze-Lefert P (2011) NLR functions in plant and animal immune systems: so far and yet so close. *Nat Immunol* **12:** 818-826.

Mes JJ, van Doorn AA, Wijbrandi J, Simons G, Cornelissen BJC, Haring MA (2000) Expression of the Fusarium resistance gene I-2 colocalizes with the site of fungal containment. *Plant J* **23:** 183-193.

Mes JJ, Wit R, Testerink CS, de Groot F, Haring MA, Cornelissen BJ (1999) Loss of avirulence and reduced pathogenicity of a Gamma-irradiated mutant of *Fusarium oxysporum* f. sp. *lycopersici*. *Phytopathology* **89:** 1131-1137.

Michielse CB, Rep M (2009) Pathogen profile update: *Fusarium oxysporum*. *Mol Plant Pathol* **10:** 311-324.

Michielse CB, van Wijk R, Reijnen L, Manders EMM, Boas S, Olivain C, Alabouvette C, Rep M (2009) The nuclear protein Sge1 of *Fusarium oxysporum* is required for parasitic growth. *PLoS Pathog* **5:** e1000637.

Nakagawa T, Suzuki T, Murata S, Nakamura S, Hino T, Maeo K, Tabata R, Kawai T, Tanaka K, Niwa Y, Watanabe Y, Nakamura K, Kimura T, Ishiguro S (2007) Improved Gateway binary vectors: high-performance vectors for creation of fusion constructs in transgenic analysis of plants. *Biosci Biotechnol Biochem* **71:** 2095-2100.

Rep M, Dekker HL, Vossen JH, de Boer AD, Houterman PM, Speijer D, Back JW, de Koster CG, Cornelissen BJC (2002) Mass spectrometric identification of Isoforms of PR proteins in xylem sap of fungus-infected tomato. *Plant Physiol* **130:** 904-917.

Rep M, van der Does HC, Meijer M, van Wijk R, Houterman PM, Dekker HL, de Koster CG, Cornelissen BJC (2004) A small, cysteine-rich protein secreted by *Fusarium oxysporum* during colonization of xylem vessels is required for I-3-mediated resistance in tomato. *Mol Microbiol* **53:** 1373-1383.

Rivas S (2012) Nuclear dynamics during plant innate immunity. *Plant Physiol* **158:** 87-94.

Rohila JS, Chen M, Cerny R, Fromm ME (2004) Improved tandem affinity purification tag and methods for isolation of protein heterocomplexes from plants. *Plant J* **38:** 172-181.

Shames SR, Finlay BB (2012) Bacterial effector interplay: a new way to view effector function. *Trends Microbiol* **20:** 214-219.

Simons G, Groenendijk J, Wijbrandi J, Reijans M, Groenen J, Diergaarde P, Van der Lee T, Bleeker M, Onstenk J, de Both M, Haring M, Mes J, Cornelissen B, Zabeau M, Vos P (1998) Dissection of the fusarium I2 gene cluster in tomato reveals six homologs and one active gene copy. *Plant Cell* **10:** 1055-1068.

Spoel SH, Dong XN (2012) How do plants achieve immunity? Defence without specialized immune cells. *Nat Rev Immunol* **12:** 89-100.

Stall RE, Walter JM (1965) Selection and inheritance of resistance in tomato to isolates of races 1 and 2 of the Fusarium wilt organism. *Phytopathology* **55:** 1213-1215.

Stergiopoulos I, de Wit PJGM (2009) Fungal Effector Proteins. *Annu Rev Phytopathol* **47:** 233-263.

Takken F, Rep M (2010) The arms race between tomato and *Fusarium oxysporum*. *Mol Plant Pathol* **11:** 309-314.

Takken FL, Van Wijk R, Michielse CB, Houterman PM, Ram AF, Cornelissen BJ (2004) A one-step method to convert vectors into binary vectors suited for Agrobacterium-mediated transformation. *Curr Genet* **45:** 242-248.

Takken FLW, Tameling WIL (2009) To Nibble at Plant Resistance Proteins. *Science* **324:** 744-746.

Tameling WIL, Elzinga SDJ, Darmin PS, Vossen JH, Takken FLW, Haring MA, Cornelissen BJC (2002) The tomato R gene products I-2 and Mi-1 are functional ATP binding proteins with ATPase activity. *Plant Cell* **14:** 2929-2939.

Tameling WIL, Nooijen C, Ludwig N, Boter M, Slootweg E, Goverse A, Shirasu K, Joosten MHAJ (2010) RanGAP2 mediates nucleocytoplasmic partitioning of the NB-LRR immune receptor Rx in the Solanaceae, thereby dictating Rx function. *Plant Cell* **22:** 4176-4194.

Tyler BM (2009) Entering and breaking: virulence effector proteins of oomycete plant pathogens. *Cell Microbiol* **11:** 13-20.

van der Does HC, Duyvesteijn RGE, Goltstein PM, van Schie CCN, Manders EMM, Cornelissen BJC, Rep M (2008) Expression of effector gene SIX1 of *Fusarium oxysporum* requires living plant cells. *Fungal Genetics and Biology* **45:** 1257-1264.

Whisson SC, Boevink PC, Moleleki L, Avrova AO, Morales JG, Gilroy EM, Armstrong MR, Grouffaud S, van West P, Chapman S, Hein I, Toth IK, Pritchard L, Birch PRJ (2007) A translocation signal for delivery of oomycete effector proteins into host plant cells. *Nature* **450:** 115.